

MIT Open Access Articles

Branching fraction of $\tau \rightarrow n K_s K_s^0$ decays

The MIT Faculty has made this article openly available. **Please share** how this access benefits you. Your story matters.

Citation: Lees, J. P. et al. "Branching Fraction of $\tau \rightarrow n K_s K_s^0$ Decays." Physical Review D 86.9 (2012). © 2012 American Physical Society

As Published: <http://dx.doi.org/10.1103/PhysRevD.86.092013>

Publisher: American Physical Society

Persistent URL: <http://hdl.handle.net/1721.1/76828>

Version: Final published version: final published article, as it appeared in a journal, conference proceedings, or other formally published context

Terms of Use: Article is made available in accordance with the publisher's policy and may be subject to US copyright law. Please refer to the publisher's site for terms of use.



Branching fraction of $\tau^- \rightarrow \pi^- K_s^0 K_s^0 (\pi^0) \nu_\tau$ decays

J. P. Lees,¹ V. Poireau,¹ V. Tisserand,¹ J. Garra Tico,² E. Grauges,² A. Palano,^{3a,3b} G. Eigen,⁴ B. Stugu,⁴ D. N. Brown,⁵ L. T. Kerth,⁵ Yu. G. Kolomensky,⁵ G. Lynch,⁵ H. Koch,⁶ T. Schroeder,⁶ D. J. Asgeirsson,⁷ C. Hearty,⁷ T. S. Mattison,⁷ J. A. McKenna,⁷ R. Y. So,⁷ A. Khan,⁸ V. E. Blinov,⁹ A. R. Buzykaev,⁹ V. P. Druzhinin,⁹ V. B. Golubev,⁹ E. A. Kravchenko,⁹ A. P. Onuchin,⁹ S. I. Serednyakov,⁹ Yu. I. Skovpen,⁹ E. P. Solodov,⁹ K. Yu. Todyshev,⁹ A. N. Yushkov,⁹ M. Bondioli,¹⁰ D. Kirkby,¹⁰ A. J. Lankford,¹⁰ M. Mandelkern,¹⁰ H. Atmacan,¹¹ J. W. Gary,¹¹ F. Liu,¹¹ O. Long,¹¹ G. M. Vitug,¹¹ C. Campagnari,¹² T. M. Hong,¹² D. Kovalskyi,¹² J. D. Richman,¹² C. A. West,¹² A. M. Eisner,¹³ J. Kroseberg,¹³ W. S. Lockman,¹³ A. J. Martinez,¹³ B. A. Schumm,¹³ A. Seiden,¹³ D. S. Chao,¹⁴ C. H. Cheng,¹⁴ B. Echenard,¹⁴ K. T. Flood,¹⁴ D. G. Hitlin,¹⁴ P. Ongmongkolkul,¹⁴ F. C. Porter,¹⁴ A. Y. Rakitin,¹⁴ R. Andreassen,¹⁵ Z. Huard,¹⁵ B. T. Meadows,¹⁵ M. D. Sokoloff,¹⁵ L. Sun,¹⁵ P. C. Bloom,¹⁶ W. T. Ford,¹⁶ A. Gaz,¹⁶ U. Nauenberg,¹⁶ J. G. Smith,¹⁶ S. R. Wagner,¹⁶ R. Ayad,^{17,*} W. H. Toki,¹⁷ B. Spaan,¹⁸ K. R. Schubert,¹⁹ R. Schwierz,¹⁹ D. Bernard,²⁰ M. Verderi,²⁰ P. J. Clark,²¹ S. Playfer,²¹ D. Bettoni,^{22a} C. Bozzi,^{22a} R. Calabrese,^{22a,22b} G. Cibinetto,^{22a,22b} E. Fioravanti,^{22a,22b} I. Garzia,^{22a,22b} E. Luppi,^{22a,22b} L. Piemontese,^{22a} V. Santoro,^{22a} R. Baldini-Ferrolì,²³ A. Calcaterra,²³ R. de Sangro,²³ G. Finocchiaro,²³ P. Patteri,²³ I. M. Peruzzi,^{23,†} M. Piccolo,²³ M. Rama,²³ A. Zallo,²³ R. Contri,^{24a,24b} E. Guido,^{24a,24b} M. Lo Vetere,^{24a,24b} M. R. Monge,^{24a,24b} S. Passaggio,^{24a} C. Patrignani,^{24a,24b} E. Robutti,^{24a} B. Bhuyan,²⁵ V. Prasad,²⁵ C. L. Lee,²⁶ M. Morii,²⁶ A. J. Edwards,²⁷ A. Adametz,²⁸ U. Uwer,²⁸ H. M. Lacker,²⁹ T. Lueck,²⁹ P. D. Dauncey,³⁰ U. Mallik,³¹ C. Chen,³² J. Cochran,³² W. T. Meyer,³² S. Prell,³² A. E. Rubin,³² A. V. Gritsan,³³ Z. J. Guo,³³ N. Arnaud,³⁴ M. Davier,³⁴ D. Derkach,³⁴ G. Grosdidier,³⁴ F. Le Diberder,³⁴ A. M. Lutz,³⁴ B. Malaescu,³⁴ P. Roudeau,³⁴ M. H. Schune,³⁴ A. Stocchi,³⁴ G. Wormser,³⁴ D. J. Lange,³⁵ D. M. Wright,³⁵ C. A. Chavez,³⁶ J. P. Coleman,³⁶ J. R. Fry,³⁶ E. Gabathuler,³⁶ D. E. Hutchcroft,³⁶ D. J. Payne,³⁶ C. Touramanis,³⁶ A. J. Bevan,³⁷ F. Di Lodovico,³⁷ R. Sacco,³⁷ M. Sigamani,³⁷ G. Cowan,³⁸ D. N. Brown,³⁹ C. L. Davis,³⁹ A. G. Denig,⁴⁰ M. Fritsch,⁴⁰ W. Gradl,⁴⁰ K. Griessinger,⁴⁰ A. Hafner,⁴⁰ E. Prencipe,⁴⁰ R. J. Barlow,^{41,‡} G. Jackson,⁴¹ G. D. Lafferty,⁴¹ E. Behn,⁴² R. Cenci,⁴² B. Hamilton,⁴² A. Jawahery,⁴² D. A. Roberts,⁴² C. Dallapiccola,⁴³ R. Cowan,⁴⁴ D. Dujmic,⁴⁴ G. Sciolla,⁴⁴ R. Cheaib,⁴⁵ D. Lindemann,⁴⁵ P. M. Patel,^{45,§} S. H. Robertson,⁴⁵ P. Biassoni,^{46a,46b} N. Neri,^{46a} F. Palombo,^{46a,46b} S. Stracka,^{46a,46b} L. Cremaldi,⁴⁷ R. Godang,^{47,||} R. Kroeger,⁴⁷ P. Sonnek,⁴⁷ D. J. Summers,⁴⁷ X. Nguyen,⁴⁸ M. Simard,⁴⁸ P. Taras,⁴⁸ G. De Nardo,^{49a,49b} D. Monorchio,^{49a,49b} G. Onorato,^{49a,49b} C. Sciacca,^{49a,49b} M. Martinelli,⁵⁰ G. Raven,⁵⁰ C. P. Jessop,⁵¹ J. M. LoSecco,⁵¹ W. F. Wang,⁵¹ K. Honscheid,⁵² R. Kass,⁵² J. Brau,⁵³ R. Frey,⁵³ N. B. Sinev,⁵³ D. Strom,⁵³ E. Torrence,⁵³ E. Feltresi,^{54a,54b} N. Gagliardi,^{54a,54b} M. Margoni,^{54a,54b} M. Morandin,^{54a} M. Posocco,^{54a} M. Rotondo,^{54a} G. Simi,^{54a} F. Simonetto,^{54a,54b} R. Stroili,^{54a,54b} S. Akar,⁵⁵ E. Ben-Haim,⁵⁵ M. Bomben,⁵⁵ G. R. Bonneaud,⁵⁵ H. Briand,⁵⁵ G. Calderini,⁵⁵ J. Chauveau,⁵⁵ O. Hamon,⁵⁵ Ph. Leruste,⁵⁵ G. Marchiori,⁵⁵ J. Ocariz,⁵⁵ S. Sitt,⁵⁵ M. Biasini,^{56a,56b} E. Manoni,^{56a,56b} S. Pacetti,^{56a,56b} A. Rossi,^{56a,56b} C. Angelini,^{57a,57b} G. Batignani,^{57a,57b} S. Bettarini,^{57a,57b} M. Carpinelli,^{57a,57b,¶} G. Casarosa,^{57a,57b} A. Cervelli,^{57a,57b} F. Forti,^{57a,57b} M. A. Giorgi,^{57a,57b} A. Lusiani,^{57a,57c} B. Oberhof,^{57a,57b} E. Paoloni,^{57a,57b} A. Perez,^{57a} G. Rizzo,^{57a,57b} J. J. Walsh,^{57a} D. Lopes Pegna,⁵⁸ J. Olsen,⁵⁸ A. J. S. Smith,⁵⁸ A. V. Telnov,⁵⁸ F. Anulli,^{59a} R. Faccini,^{59a,59b} F. Ferrarotto,^{59a} F. Ferroni,^{59a,59b} M. Gaspero,^{59a,59b} L. Li Gioi,^{59a} M. A. Mazzoni,^{59a} G. Piredda,^{59a} C. Büniger,⁶⁰ O. Grünberg,⁶⁰ T. Hartmann,⁶⁰ T. Leddig,⁶⁰ C. Voß,⁶⁰ R. Waldi,⁶⁰ T. Adye,⁶¹ E. O. Olaiya,⁶¹ F. F. Wilson,⁶¹ S. Emery,⁶² G. Hamel de Monchenault,⁶² G. Vasseur,⁶² Ch. Yèche,⁶² D. Aston,⁶³ D. J. Bard,⁶³ R. Bartoldus,⁶³ J. F. Benitez,⁶³ C. Cartaro,⁶³ M. R. Convery,⁶³ J. Dorfan,⁶³ G. P. Dubois-Felsmann,⁶³ W. Dunwoodie,⁶³ M. Ebert,⁶³ R. C. Field,⁶³ M. Franco Sevilla,⁶³ B. G. Fulsom,⁶³ A. M. Gabareen,⁶³ M. T. Graham,⁶³ P. Grenier,⁶³ C. Hast,⁶³ W. R. Innes,⁶³ M. H. Kelsey,⁶³ P. Kim,⁶³ M. L. Kocian,⁶³ D. W. G. S. Leith,⁶³ P. Lewis,⁶³ B. Lindquist,⁶³ S. Luitz,⁶³ V. Luth,⁶³ H. L. Lynch,⁶³ D. B. MacFarlane,⁶³ D. R. Muller,⁶³ H. Neal,⁶³ S. Nelson,⁶³ M. Perl,⁶³ T. Pulliam,⁶³ B. N. Ratcliff,⁶³ A. Roodman,⁶³ A. A. Salnikov,⁶³ R. H. Schindler,⁶³ A. Snyder,⁶³ D. Su,⁶³ M. K. Sullivan,⁶³ J. Va'vra,⁶³ A. P. Wagner,⁶³ W. J. Wisniewski,⁶³ M. Wittgen,⁶³ D. H. Wright,⁶³ H. W. Wulsin,⁶³ C. C. Young,⁶³ V. Ziegler,⁶³ W. Park,⁶⁴ M. V. Purohit,⁶⁴ R. M. White,⁶⁴ J. R. Wilson,⁶⁴ A. Randle-Conde,⁶⁵ S. J. Sekula,⁶⁵ M. Bellis,⁶⁶ P. R. Burchat,⁶⁶ T. S. Miyashita,⁶⁶ E. M. T. Puccio,⁶⁶ M. S. Alam,⁶⁷ J. A. Ernst,⁶⁷ R. Gorodeisky,⁶⁸ N. Guttman,⁶⁸ D. R. Peimer,⁶⁸ A. Soffer,⁶⁸ P. Lund,⁶⁹ S. M. Spanier,⁶⁹ J. L. Ritchie,⁷⁰ A. M. Ruland,⁷⁰ R. F. Schwitters,⁷⁰ B. C. Wray,⁷⁰ J. M. Izen,⁷¹ X. C. Lou,⁷¹ F. Bianchi,^{72a,72b} D. Gamba,^{72a,72b} S. Zambito,^{72a,72b} L. Lancieri,^{73a,73b} L. Vitale,^{73a,73b} F. Martinez-Vidal,⁷⁴ A. Oyanguren,⁷⁴ P. Villanueva-Perez,⁷⁴ H. Ahmed,⁷⁵ J. Albert,⁷⁵ Sw. Banerjee,⁷⁵ F. U. Bernlochner,⁷⁵ H. H. F. Choi,⁷⁵ G. J. King,⁷⁵ R. Kowalewski,⁷⁵ M. J. Lewczuk,⁷⁵ I. M. Nugent,⁷⁵ J. M. Roney,⁷⁵ R. J. Sobie,⁷⁵ N. Tasneem,⁷⁵ T. J. Gershon,⁷⁶ P. F. Harrison,⁷⁶ T. E. Latham,⁷⁶ H. R. Band,⁷⁷ S. Dasu,⁷⁷ Y. Pan,⁷⁷ R. Prepost,⁷⁷ and S. L. Wu⁷⁷

- ¹Laboratoire d'Annecy-le-Vieux de Physique des Particules (LAPP), Université de Savoie, CNRS/IN2P3, F-74941 Annecy-Le-Vieux, France
- ²Departament ECM, Facultat de Física, Universitat de Barcelona, E-08028 Barcelona, Spain
- ^{3a}INFN Sezione di Bari, I-70126 Bari, Italy
- ^{3b}Dipartimento di Fisica, Università di Bari, I-70126 Bari, Italy
- ⁴Institute of Physics, University of Bergen, N-5007 Bergen, Norway
- ⁵Lawrence Berkeley National Laboratory and University of California, Berkeley, California 94720, USA
- ⁶Institut für Experimentalphysik I, Ruhr Universität Bochum, D-44780 Bochum, Germany
- ⁷University of British Columbia, Vancouver, British Columbia, Canada V6T 1Z1
- ⁸Brunel University, Uxbridge, Middlesex UB8 3PH, United Kingdom
- ⁹Budker Institute of Nuclear Physics, Novosibirsk 630090, Russia
- ¹⁰University of California at Irvine, Irvine, California 92697, USA
- ¹¹University of California at Riverside, Riverside, California 92521, USA
- ¹²University of California at Santa Barbara, Santa Barbara, California 93106, USA
- ¹³Institute for Particle Physics, University of California at Santa Cruz, Santa Cruz, California 95064, USA
- ¹⁴California Institute of Technology, Pasadena, California 91125, USA
- ¹⁵University of Cincinnati, Cincinnati, Ohio 45221, USA
- ¹⁶University of Colorado, Boulder, Colorado 80309, USA
- ¹⁷Colorado State University, Fort Collins, Colorado 80523, USA
- ¹⁸Fakultät Physik, Technische Universität Dortmund, D-44221 Dortmund, Germany
- ¹⁹Institut für Kern- und Teilchenphysik, Technische Universität Dresden, D-01062 Dresden, Germany
- ²⁰Laboratoire Leprince-Ringuet, Ecole Polytechnique, CNRS/IN2P3, F-91128 Palaiseau, France
- ²¹University of Edinburgh, Edinburgh EH9 3JZ, United Kingdom
- ^{22a}INFN Sezione di Ferrara, I-44100 Ferrara, Italy
- ^{22b}Dipartimento di Fisica, Università di Ferrara, I-44100 Ferrara, Italy
- ²³INFN Laboratori Nazionali di Frascati, I-00044 Frascati, Italy
- ^{24a}INFN Sezione di Genova, I-16146 Genova, Italy
- ^{24b}Dipartimento di Fisica, Università di Genova, I-16146 Genova, Italy
- ²⁵Indian Institute of Technology Guwahati, Guwahati, Assam 781039, India
- ²⁶Harvard University, Cambridge, Massachusetts 02138, USA
- ²⁷Harvey Mudd College, Claremont, California 91711, USA
- ²⁸Physikalisches Institut, Universität Heidelberg, Philosophenweg 12, D-69120 Heidelberg, Germany
- ²⁹Institut für Physik, Humboldt-Universität zu Berlin, Newtonstraße 15, D-12489 Berlin, Germany
- ³⁰Imperial College London, London SW7 2AZ, United Kingdom
- ³¹University of Iowa, Iowa, Iowa 52242, USA
- ³²Iowa State University, Ames, Iowa 50011-3160, USA
- ³³Johns Hopkins University, Baltimore, Maryland 21218, USA
- ³⁴Laboratoire de l'Accélérateur Linéaire, IN2P3/CNRS et Université Paris-Sud 11, Centre Scientifique d'Orsay, Boîte Postale 34, F-91898 Orsay Cedex, France
- ³⁵Lawrence Livermore National Laboratory, Livermore, California 94550, USA
- ³⁶University of Liverpool, Liverpool L69 7ZE, United Kingdom
- ³⁷Queen Mary, University of London, London E1 4NS, United Kingdom
- ³⁸Royal Holloway and Bedford New College, University of London, Egham, Surrey TW20 0EX, United Kingdom
- ³⁹University of Louisville, Louisville, Kentucky 40292, USA
- ⁴⁰Institut für Kernphysik, Johannes Gutenberg-Universität Mainz, D-55099 Mainz, Germany
- ⁴¹University of Manchester, Manchester M13 9PL, United Kingdom
- ⁴²University of Maryland, College Park, Maryland 20742, USA
- ⁴³University of Massachusetts, Amherst, Massachusetts 01003, USA
- ⁴⁴Laboratory for Nuclear Science, Massachusetts Institute of Technology, Cambridge, Massachusetts 02139, USA
- ⁴⁵McGill University, Montréal, Québec, Canada H3A 2T8
- ^{46a}INFN Sezione di Milano, I-20133 Milano, Italy
- ^{46b}Dipartimento di Fisica, Università di Milano, I-20133 Milano, Italy
- ⁴⁷University of Mississippi, University, Mississippi 38677, USA
- ⁴⁸Université de Montréal, Physique des Particules, Montréal, Québec, Canada H3C 3J7
- ^{49a}INFN Sezione di Napoli, I-80126 Napoli, Italy
- ^{49b}Dipartimento di Scienze Fisiche, Università di Napoli Federico II, I-80126 Napoli, Italy
- ⁵⁰NIKHEF, National Institute for Nuclear Physics and High Energy Physics, NL-1009 DB Amsterdam, The Netherlands
- ⁵¹University of Notre Dame, Notre Dame, Indiana 46556, USA
- ⁵²Ohio State University, Columbus, Ohio 43210, USA
- ⁵³University of Oregon, Eugene, Oregon 97403, USA
- ^{54a}INFN Sezione di Padova, I-35131 Padova, Italy

- ^{54b}*Dipartimento di Fisica, Università di Padova, I-35131 Padova, Italy*
- ⁵⁵*Laboratoire de Physique Nucléaire et de Hautes Energies, IN2P3/CNRS, Université Pierre et Marie Curie-Paris6, Université Denis Diderot-Paris7, F-75252 Paris, France*
- ^{56a}*INFN Sezione di Perugia, I-06100 Perugia, Italy*
- ^{56b}*Dipartimento di Fisica, Università di Perugia, I-06100 Perugia, Italy*
- ^{57a}*INFN Sezione di Pisa; I-56127 Pisa, Italy*
- ^{57b}*Dipartimento di Fisica, Università di Pisa; I-56127 Pisa, Italy*
- ^{57c}*Scuola Normale Superiore di Pisa, I-56127 Pisa, Italy*
- ⁵⁸*Princeton University, Princeton, New Jersey 08544, USA*
- ^{59a}*INFN Sezione di Roma; I-00185 Roma, Italy*
- ^{59b}*Dipartimento di Fisica, Università di Roma La Sapienza, I-00185 Roma, Italy*
- ⁶⁰*Universität Rostock, D-18051 Rostock, Germany*
- ⁶¹*Rutherford Appleton Laboratory, Chilton, Didcot, Oxon OX11 0QX, United Kingdom*
- ⁶²*CEA, Irfu, SPP, Centre de Saclay, F-91191 Gif-sur-Yvette, France*
- ⁶³*SLAC National Accelerator Laboratory, Stanford, California 94309, USA*
- ⁶⁴*University of South Carolina, Columbia, South Carolina 29208, USA*
- ⁶⁵*Southern Methodist University, Dallas, Texas 75275, USA*
- ⁶⁶*Stanford University, Stanford, California 94305-4060, USA*
- ⁶⁷*State University of New York, Albany, New York 12222, USA*
- ⁶⁸*Tel Aviv University, School of Physics and Astronomy, Tel Aviv 69978, Israel*
- ⁶⁹*University of Tennessee, Knoxville, Tennessee 37996, USA*
- ⁷⁰*University of Texas at Austin, Austin, Texas 78712, USA*
- ⁷¹*University of Texas at Dallas, Richardson, Texas 75083, USA*
- ^{72a}*INFN Sezione di Torino; I-10125 Torino, Italy*
- ^{72b}*Dipartimento di Fisica Sperimentale, Università di Torino, I-10125 Torino, Italy*
- ^{73a}*INFN Sezione di Trieste; I-34127 Trieste, Italy*
- ^{73b}*Dipartimento di Fisica, Università di Trieste, I-34127 Trieste, Italy*
- ⁷⁴*IFIC, Universitat de Valencia-CSIC, E-46071 Valencia, Spain*
- ⁷⁵*University of Victoria, Victoria, British Columbia, Canada V8W 3P6*
- ⁷⁶*Department of Physics, University of Warwick, Coventry CV4 7AL, United Kingdom*
- ⁷⁷*University of Wisconsin, Madison, Wisconsin 53706, USA*

(Received 2 August 2012; published 26 November 2012)

We present a study of $\tau^- \rightarrow \pi^- K_S^0 K_S^0(\pi^0)\nu_\tau$ and $\tau^- \rightarrow K^- K_S^0 K_S^0(\pi^0)\nu_\tau$ decays using a data set of 430 million τ lepton pairs, corresponding to an integrated luminosity of 468 fb^{-1} , collected with the *BABAR* detector at the PEP-II asymmetric energy e^+e^- storage rings. We measure branching fractions of $(2.31 \pm 0.04 \pm 0.08) \times 10^{-4}$ and $(1.60 \pm 0.20 \pm 0.22) \times 10^{-5}$ for the $\tau^- \rightarrow \pi^- K_S^0 K_S^0 \nu_\tau$ and $\tau^- \rightarrow \pi^- K_S^0 K_S^0 \pi^0 \nu_\tau$ decays, respectively. We find no evidence for $\tau^- \rightarrow K^- K_S^0 K_S^0 \nu_\tau$ and $\tau^- \rightarrow K^- K_S^0 K_S^0 \pi^0 \nu_\tau$ decays and place upper limits on the branching fractions of 6.3×10^{-7} and 4.0×10^{-7} at the 90% confidence level.

DOI: [10.1103/PhysRevD.86.092013](https://doi.org/10.1103/PhysRevD.86.092013)

PACS numbers: 13.35.Dx, 14.60.Fg

The τ lepton can be used as a high-precision probe of the Standard Model and models of new physics. A recent *BABAR* paper, for example, presented a search for CP violation by measuring the decay-rate asymmetry of $\tau^- \rightarrow \pi^- K_S^0 \nu_\tau$ decays [1]. One of the backgrounds in that

analysis is $\tau^- \rightarrow \pi^- K_S^0 K_S^0 \nu_\tau$, which has a large uncertainty in the branching fraction [2]. The uncertainty in the background from $\tau^- \rightarrow \pi^- K_S^0 K_S^0 \nu_\tau$ decays was not a limitation of the decay-rate asymmetry measurement, but an improved measurement of the branching fraction and an understanding of the decay dynamics will be required for a future measurement at a high-luminosity B -factory.

This paper presents measurements of the branching fractions of $\tau^- \rightarrow \pi^- K_S^0 K_S^0(\pi^0)\nu_\tau$ decays and the first search for $\tau^- \rightarrow K^- K_S^0 K_S^0(\pi^0)\nu_\tau$ decays. In this work we use the $K_S^0 \rightarrow \pi^+\pi^-$ decay mode. Here and throughout the paper, charge conjugation is implied.

Previously, ALEPH and CLEO measured the $\tau^- \rightarrow \pi^- K_S^0 K_S^0 \nu_\tau$ branching fraction to be $(2.6 \pm 1.0 \pm 0.5) \times 10^{-4}$ [3] and $(2.3 \pm 0.5 \pm 0.3) \times 10^{-4}$ [4], respectively.

*Present address: University of Tabuk, Tabuk 71491, Saudi Arabia.

†Also with Università di Perugia, Dipartimento di Fisica, Perugia, Italy.

‡Present address: University of Huddersfield, Huddersfield HD1 3DH, United Kingdom.

§Deceased.

||Present address: University of South Alabama, Mobile, Alabama 36688, USA.

¶Also with Università di Sassari, Sassari, Italy.

ALEPH set an upper limit on the $\tau^- \rightarrow \pi^- K_S^0 K_S^0 \pi^0 \nu_\tau$ branching fraction of 2×10^{-4} at the 95% confidence level [3].

The present analysis uses data recorded by the *BABAR* detector at the PEP-II asymmetric-energy e^+e^- collider, operated at center-of-mass (CM) energies of 10.58 and 10.54 GeV at the SLAC National Accelerator Laboratory. The *BABAR* detector is described in detail in Ref. [5]. In particular, charged particle momenta are measured with a five-layer double-sided silicon vertex tracker and a 40-layer drift chamber, both within a 1.5 T superconducting solenoidal magnet. Charged kaons and pions are separated by ionization (dE/dx) measurements in the silicon vertex detector and the drift chamber in combination with an internally reflecting Cherenkov detector. An electromagnetic calorimeter made of thallium-doped cesium iodide crystals provides energy measurements for electrons and photons, and an instrumented flux return detector identifies muons. Based on an integrated luminosity of 468 fb^{-1} , the data sample contains approximately 430 million τ -pair events.

Simulated event samples are used to estimate the selection efficiency and purity of the data sample. The production of τ pairs is simulated with the KK2F Monte Carlo (MC) event generator [6]. Subsequent decays of the τ lepton, continuum $q\bar{q}$ events (where $q = u, d, s, c$), and final-state radiative effects are modeled with Tauola [7] and EvtGen [8], JETSET [9], and PHOTOS [10], respectively. Passage of the particles through the detector is simulated by Geant4 [11].

The $\tau^- \rightarrow \pi^- K_S^0 K_S^0 \nu_\tau$ decay is simulated with Tauola using $\tau^- \rightarrow K^{*-} K^0 \nu_\tau$. The $\tau^- \rightarrow \pi^- K_S^0 K_S^0 \pi^0 \nu_\tau$ decay is simulated with EvtGen using $\tau^- \rightarrow K^{*-} K^0 \pi^0 \nu_\tau$ and $\tau^- \rightarrow K^{*0} K^0 \pi^- \nu_\tau$. As we later show, the $\tau^- \rightarrow K^{*-} K^0 \nu_\tau$ and $\tau^- \rightarrow K^{*0} K^0 \pi^- \nu_\tau$ have a $K^*(892)$ meson that is observed in the $\pi^- K_S^0$ channel, and the $\tau^- \rightarrow K^{*0} K^0 \pi^- \nu_\tau$ has a $K^*(892)$ meson that is observed in the $\pi^0 K_S^0$ channel.

The τ pair is produced back-to-back in the e^+e^- CM frame. As a result, the decay products of the two τ leptons can be separated from each other by dividing the event into two hemispheres—referred to later as the “signal” hemisphere and the “tag” hemisphere—using the plane perpendicular to the event thrust axis [12]. The event thrust axis is calculated using all charged particles and all photon candidates in the entire event.

We select events with one prompt track and two $K_S^0 \rightarrow \pi^+ \pi^-$ candidates reconstructed in the signal hemisphere, and exactly one oppositely charged prompt track in the tag hemisphere. All tracks are required to have the components of momentum transverse to the e^- beam axis be greater than 0.1 GeV/c in the laboratory frame. A prompt track is defined to be a track with its point of closest approach to the beam spot being less than 1.5 cm in the plane transverse to the e^- beam axis and less than 2.5 cm in the direction of

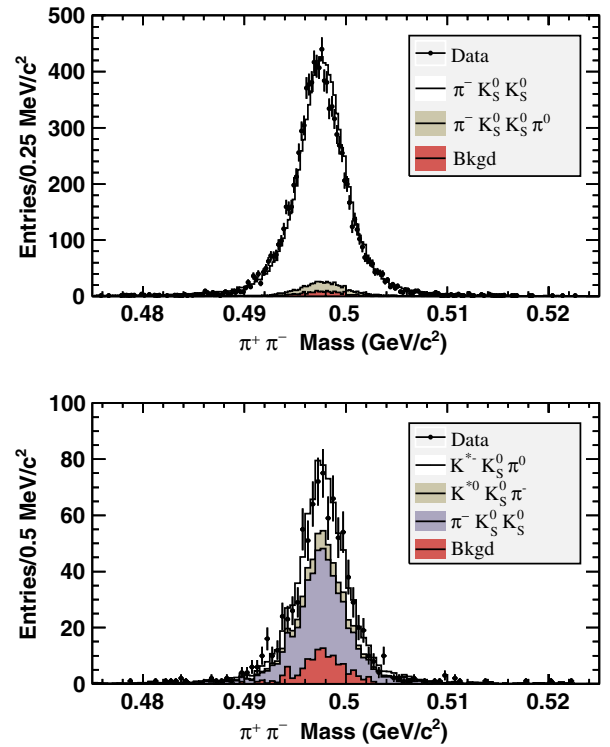


FIG. 1 (color online). The invariant mass of the two $K_S^0 \rightarrow \pi^+ \pi^-$ candidates in the $\tau^- \rightarrow \pi^- K_S^0 K_S^0 \nu_\tau$ (top) and $\tau^- \rightarrow \pi^- K_S^0 K_S^0 \pi^0 \nu_\tau$ (bottom) samples after all selection criteria have been applied. The points are data and the histograms are the prediction of the Monte Carlo simulation. For both plots, the white histogram represents $\tau^- \rightarrow K^{*-} K^0 \nu_\tau$ decays, and the blue (medium shaded) and beige (light shaded) histogram shows the $\tau^- \rightarrow K^{*0} K^0 \pi^0 \nu_\tau$ and $\tau^- \rightarrow K^{*0} K^0 \pi^- \nu_\tau$ ($\tau^- \rightarrow \pi^- K_S^0 K_S^0 \pi^0 \nu_\tau$) decays, respectively. The red (dark shaded) histogram is the $q\bar{q}$ background.

the e^- beam axis. A K_S^0 candidate is defined as a pair of oppositely charged tracks where neither track is identified as a prompt track. The invariant mass of the K_S^0 candidate is required to be between 0.475 and 0.525 GeV/c^2 (see Fig. 1). Furthermore, the distance between the beam spot and the $\pi^+ \pi^-$ vertex must be at least three times its uncertainty (the di-pion pair will be referred to as the “ K_S^0 candidate daughters”).

The charged hadron must be identified as a charged pion or a charged kaon. The efficiency for selecting charged pions and kaons is approximately 95 and 90%, respectively. The probability of misidentifying a charged pion (kaon) as a charged kaon (pion) is estimated to be 1% (5%).

The charged pion and kaon samples are divided into samples with zero and one π^0 mesons. Events with two or more π^0 mesons are rejected. The π^0 candidate is reconstructed from two clusters of energy deposits in the electromagnetic calorimeter that have no associated tracks. The energy of each cluster is required to be greater than 30 MeV in the laboratory frame, and the invariant mass of the two clusters must be between 0.115 and 0.150 GeV/c^2 .

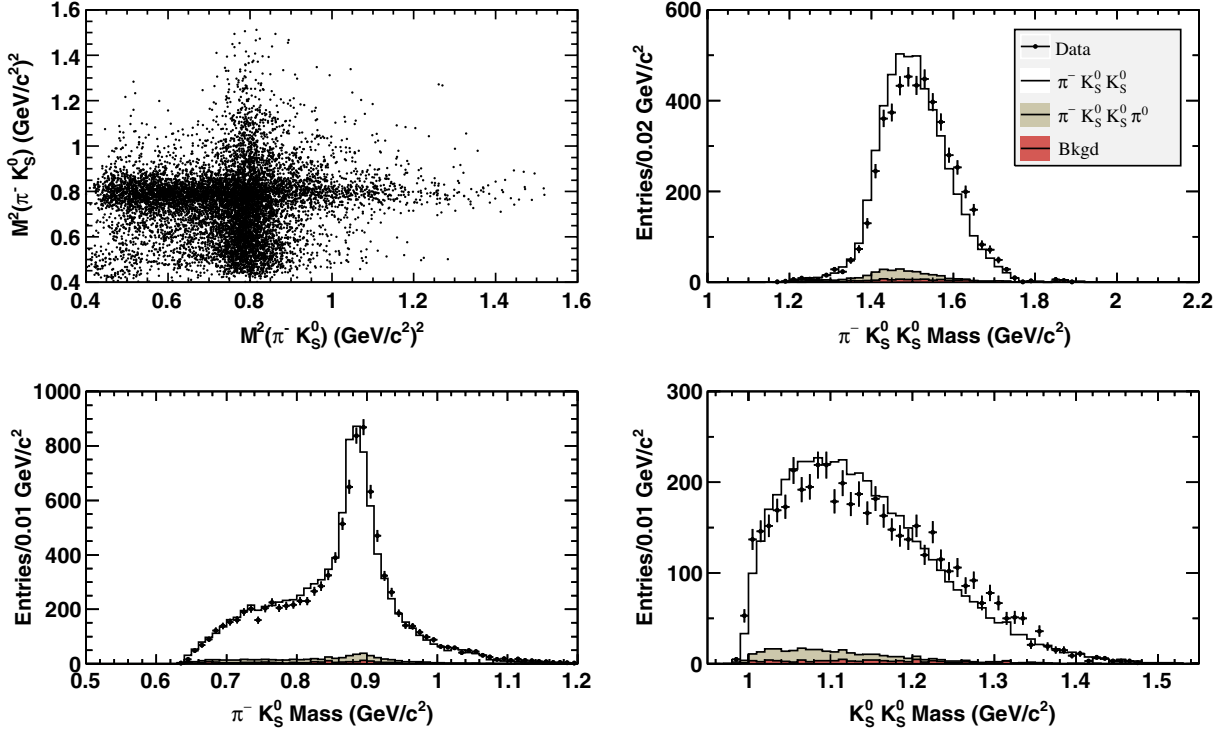


FIG. 2 (color online). The Dalitz plot of the $(\pi^- K_S^0)$ system, and the $(\pi^- K_S^0 K_S^0)$, $(\pi^- K_S^0)$ and $(K_S^0 K_S^0)$ invariant mass distributions for events that pass the $\tau^- \rightarrow \pi^- K_S^0 K_S^0 \nu_\tau$ selection criteria. The invariant mass requirement is not required for the plot of the $(\pi^- K_S^0 K_S^0)$ invariant mass. There are two entries per event in the Dalitz plot and in the $(\pi^- K_S^0)$ mass plot. The points are data and the histograms are the prediction of the Monte Carlo simulation. The signal decays are represented by the white histogram ($\tau^- \rightarrow K^{*0} K^0 \nu_\tau$). The beige (light shaded) histogram shows the $\tau^- \rightarrow K^{*0} K^0 \pi^0 \nu_\tau$ and $\tau^- \rightarrow K^{*0} K^0 \pi^- \nu_\tau$ ($\tau^- \rightarrow \pi^- K_S^0 K_S^0 \pi^0 \nu_\tau$) decays. The red (dark shaded) histogram is the $q\bar{q}$ background. The mass plots use $\tau^- \rightarrow \pi^- K_S^0 K_S^0 \nu_\tau$ events that have been weighted based on the Dalitz plot distributions in the top left plot.

The clusters in the electromagnetic calorimeter that are not associated with a π^0 candidate are ignored in the analysis.

To reduce backgrounds from non- τ pair events, we require that the momentum of the charged particle in the tag hemisphere is less than 4 GeV/c in the CM frame and be identified as either an electron or a muon. For momenta above 1 GeV/c in the laboratory frame, electrons and muons are identified with efficiencies of approximately 92 and 70%, respectively [13]. We also require the magnitude of the event thrust to be between 0.90 and 0.995.

The invariant mass of the charged hadron and the two K_S^0 mesons is required to be less than 1.8 GeV/c². For $\tau^- \rightarrow \pi^- K_S^0 K_S^0 \pi^0 \nu_\tau$ decays, we do not include the π^0 in the mass calculation. The $\pi^- K_S^0 K_S^0$ invariant mass is shown in Figs. 2 and 3. The $\pi^- K_S^0 K_S^0 \pi^0$ invariant mass is also shown in Fig. 3. We also require the pseudomass to be less than 1.9 and 2.1 GeV/c² for the $\tau^- \rightarrow \pi^- K_S^0 K_S^0 \nu_\tau$ and $\tau^- \rightarrow \pi^- K_S^0 K_S^0 \pi^0 \nu_\tau$ samples, respectively (the π^0 meson is included in the pseudomass calculation). The pseudomass is defined to be $M_{\text{pseudo}} = \sqrt{M_h^2 + 2(\sqrt{s} - E_h)(E_h - P_h)}$ where E_h and P_h are the energy and magnitude of the momentum of the hadronic final state in the laboratory frame [14].

The invariant mass distribution predicted by the MC for the hadronic final state particles and for their combinations does not perfectly describe the data. In particular, the peak of the $(\pi^- K_S^0 K_S^0)$ invariant mass distribution in the MC is found to peak approximately 5% lower than the peak observed in the data. To improve the modeling of the data we have weighted the $\tau^- \rightarrow \pi^- K_S^0 K_S^0 \nu_\tau$ in Tauola using the Dalitz plot distribution for the $\pi^- K_S^0$ invariant mass (shown for the data sample in Fig. 2). The weighting function is from a two-dimensional (9×9) matrix using $M^2(\pi^- K_S^0)$ with both $\pi^- K_S^0$ combinations (the matrix is constructed to be symmetric). The weighted events are used in all the mass plots and we observe an improvement in the modeling of the data.

The branching fractions of the two charged pion modes are determined simultaneously to take into account the cross feed of each decay mode into the other sample. The branching fraction is

$$B_j = \sum_i \epsilon_{ji}^{-1} (N_i^{\text{data}} - N_i^{\text{bkgd}}) / (2N_{\tau\tau})$$

where j represents the $\tau^- \rightarrow \pi^- K_S^0 K_S^0 \nu_\tau$ and $\tau^- \rightarrow \pi^- K_S^0 K_S^0 \pi^0 \nu_\tau$ decay modes; i represents the $(\pi^- K_S^0 K_S^0)$ or $(\pi^- K_S^0 K_S^0 \pi^0)$ reconstruction modes; N_i^{data} and N_i^{bkgd} are

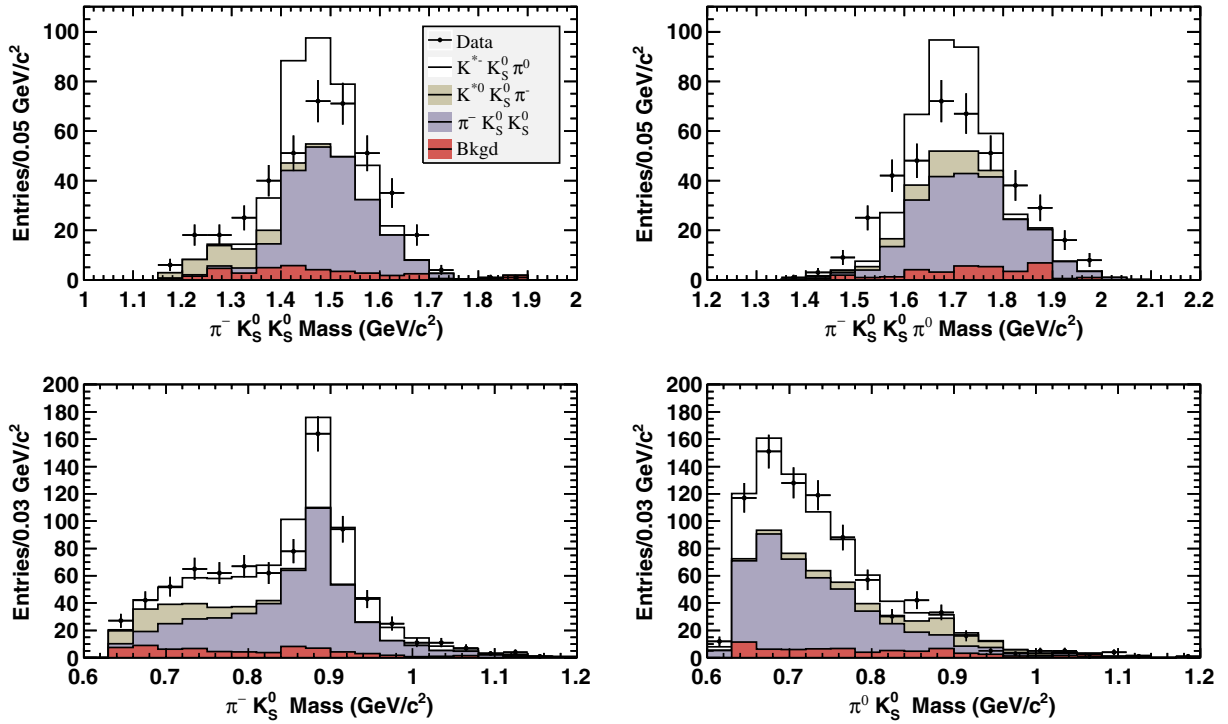


FIG. 3 (color online). The $(\pi^- K_S^0 K_S^0)$, $(\pi^- K_S^0 K_S^0 \pi^0)$, $(\pi^- K_S^0)$, and $(\pi^0 K_S^0)$ invariant mass distributions that pass the $\tau^- \rightarrow \pi^- K_S^0 K_S^0 \pi^0 \nu_\tau$ selection criteria [except for the plot of the $(\pi^- K_S^0 K_S^0)$ invariant mass where the selection requirement on the mass is not included]. There are two entries per event in the $(\pi^- K_S^0)$ and $(\pi^0 K_S^0)$ mass plots. The points are data and the histograms are the predictions of the Monte Carlo simulation. The two signal channels are shown in the white ($\tau^- \rightarrow K^{*-} K^0 \pi^0 \nu_\tau$) and beige (light shaded) ($\tau^- \rightarrow K^{*0} K^0 \pi^- \nu_\tau$) histograms. The dark blue (medium shaded) histogram is $\tau^- \rightarrow \pi^- K_S^0 K_S^0 \nu_\tau$ ($\tau^- \rightarrow K^{*-} K^0 \nu_\tau$) decays. The red (dark shaded) histogram is the $q\bar{q}$ background. The mass plots use $\tau^- \rightarrow \pi^- K_S^0 K_S^0 \nu_\tau$ events that have been weighted based on the Dalitz plot distributions shown in Fig. 2.

the number of data and background events in the i th data sample; ϵ^{-1} is the inverse of the selection efficiency matrix (ϵ_{ij} is the probability to select an event of type j with the selection criteria i); and $N_{\tau\tau}$ is the number of τ -pair candidates determined from the integrated luminosity and the $e^-e^- \rightarrow$ cross section.

The columns in Table I give the number of data and background events for each reconstruction mode. Table I also gives the selection efficiency matrix, where the horizontal row gives the efficiency for selecting the true decay for each reconstructed mode. For example, the efficiency for selecting a true $\tau^- \rightarrow \pi^- K_S^0 K_S^0 \nu_\tau$ decay is

TABLE I. Results for the charged pion decays. The background events are primarily $q\bar{q}$ events.

Decay mode	$\tau^- \rightarrow \pi^- K_S^0 K_S^0 \nu_\tau$	$\tau^- \rightarrow \pi^- K_S^0 K_S^0 \pi^0 \nu_\tau$
Branching fraction	$(2.31 \pm 0.04 \pm 0.08) \times 10^{-4}$	$(1.60 \pm 0.20 \pm 0.22) \times 10^{-5}$
Events		
Data	4985	409
Estimated background	98 ± 17	35 ± 7
Selection efficiency		
$\tau^- \rightarrow \pi^- K_S^0 K_S^0 \nu_\tau$	$(4.93 \pm 0.02)\%$	$(0.21 \pm 0.01)\%$
$\tau^- \rightarrow \pi^- K_S^0 K_S^0 \pi^0 \nu_\tau$	$(3.04 \pm 0.10)\%$	$(2.65 \pm 0.09)\%$
Fractional systematic errors		
Selection efficiency	0.008	0.12
Background	0.004	0.04
Common systematics	0.034	0.03
Total	0.035	0.13

$(4.93 \pm 0.02)\%$ and $(0.21 \pm 0.01)\%$ with the $(\pi^- K_S^0 K_S^0)$ and $(\pi^- K_S^0 K_S^0 \pi^0)$ selection criteria, respectively.

We measure the $\tau^- \rightarrow \pi^- K_S^0 K_S^0 \nu_\tau$ and $\tau^- \rightarrow \pi^- K_S^0 K_S^0 \pi^0 \nu_\tau$ branching fractions to be

$$B(\tau^- \rightarrow \pi^- K_S^0 K_S^0 \nu_\tau) = (2.31 \pm 0.04 \pm 0.08) \times 10^{-4},$$

$$B(\tau^- \rightarrow \pi^- K_S^0 K_S^0 \pi^0 \nu_\tau) = (1.60 \pm 0.20 \pm 0.22) \times 10^{-5},$$

where the first error is statistical and the second is systematic. The statistical correlation parameter for the two measurements is found to be -0.21 . The results have been corrected for the $K_S^0 \rightarrow \pi^+ \pi^-$ branching fraction [2].

The systematic uncertainties (see Table I) are divided into the selection efficiency, background, and common systematic components. The uncertainties on the elements of the efficiency matrix only include the errors specific to that decay and those selection criteria. Uncertainties that are common to all matrix elements are included in the common systematic errors.

The efficiency for selecting $\tau^- \rightarrow \pi^- K_S^0 K_S^0 \nu_\tau$ events is found to be $(4.93 \pm 0.02)\%$ and $(0.21 \pm 0.01)\%$ for the samples with zero and one π^0 candidate, respectively. The uncertainty on the first efficiency is from the MC statistical error. The uncertainty on the second efficiency also includes the MC statistical error and an error that takes into account the uncertainty for finding a fake π^0 meson in $\tau^- \rightarrow \pi^- K_S^0 K_S^0 \nu_\tau$ decays. The uncertainty for finding a fake π^0 is estimated to be 6% and is determined by comparing the number of $\tau^- \rightarrow \pi^- K_S^0 K_S^0 \nu_\tau$ decays that have two neutral clusters in the data and MC samples where the invariant mass of the two neutral clusters must not be near the π^0 mass.

The efficiency for selecting $\tau^- \rightarrow \pi^- K_S^0 K_S^0 \pi^0 \nu_\tau$ events is found to be $(3.04 \pm 0.10)\%$ and $(2.65 \pm 0.09)\%$ for the samples with zero and one π^0 candidate, respectively. The uncertainties include the MC statistical error and an uncertainty for the π^0 identification. The uncertainty for identifying a π^0 meson is estimated to be 3% based on studies with tau lepton and D meson data and MC control samples. We observe that the efficiency for selecting $\tau^- \rightarrow \pi^- K_S^0 K_S^0 \pi^0 \nu_\tau$ decays with and without a π^0 is approximately equal, and hence we assign a 3% uncertainty on the efficiency for selecting $\tau^- \rightarrow \pi^- K_S^0 K_S^0 \pi^0 \nu_\tau$ decays without reconstructing the π^0 meson.

The background in the charged pion modes is predicted by the MC simulation to be entirely from $e^+ e^- \rightarrow q\bar{q}$ events. The background in the charged kaon modes is cross fed from the charged pion modes where a charged pion is misidentified as the charged kaon. The background in the charged pion sample is confirmed with data and MC simulation control samples. The control samples are created using the nominal selection criteria except that the invariant mass and pseudomass requirements are reversed to eliminate the τ -pair events and enhance $q\bar{q}$ events. The ratio of selected events in the data to MC control samples is

found to be consistent with unity within 15% for both $\tau^- \rightarrow \pi^- K_S^0 K_S^0 \nu_\tau$ and $\tau^- \rightarrow \pi^- K_S^0 K_S^0 \pi^0 \nu_\tau$ samples. The 15% value is added to the MC statistical uncertainty of the number of background events.

A number of systematic uncertainties are common to both the $\tau^- \rightarrow \pi^- K_S^0 K_S^0 \nu_\tau$ and $\tau^- \rightarrow \pi^- K_S^0 K_S^0 \pi^0 \nu_\tau$ branching fractions' measurements. They can be categorized into two components: tracking and particle identification reconstruction uncertainties, and topological selection uncertainties.

The tracking and particle identification reconstruction uncertainties include the uncertainty on the track reconstruction efficiency (0.5%). They also include the uncertainties on the efficiencies of the particle identification algorithms: lepton identification (combined electron and muon) (1.6%), charged pion particle identification (0.5%), and K_S^0 identification (1.8% for two K_S^0). The particle identification algorithms used in this work are based on standard *BABAR* routines and the uncertainties are determined using control data and MC samples [5,15]. The uncertainty on the efficiency for selecting π^0 mesons is included in the elements of the selection efficiency matrix.

The topological selection uncertainties include a 2% uncertainty associated with the topological selection criteria that impose requirements that the prompt tracks be associated with the primary vertex. Also included is the uncertainty in the product of the luminosity multiplied by the $e^+ e^- \rightarrow \tau^+ \tau^-$ cross section (1%). If the weighting of the invariant mass distribution of the $\tau^- \rightarrow \pi^- K_S^0 K_S^0 \nu_\tau$ MC decays is not included (or another weighting scheme is used), we find the change in the measured branching ratios to be negligible compared with the other systematic uncertainties.

In Fig. 2 we plot the $(\pi^- K_S^0 K_S^0)$, $(\pi^- K_S^0)$, and $(K_S^0 K_S^0)$ invariant mass distributions. The contribution of the $K^*(892)$ resonance ($K^* \rightarrow \pi^- K_S^0$) is observed in the $(\pi^- K_S^0)$ invariant mass plot and the Dalitz plot in Fig. 2.

The $\tau^- \rightarrow \pi^- K_S^0 K_S^0 \nu_\tau$ branching fraction is in good agreement with the previous measurements of $(2.6 \pm 1.0 \pm 0.5) \times 10^{-4}$ [3] and $(2.3 \pm 0.5 \pm 0.3) \times 10^{-4}$ [4]. The theoretical prediction for the $\tau^- \rightarrow \pi^- K_S^0 K_S^0 \nu_\tau$ branching fraction is 4.8×10^{-4} [16]. Decays involving a pion and two kaon mesons can have contributions from both axial and vector currents at the same time, and the vector contribution for $\tau^- \rightarrow \pi^- K_S^0 K_S^0 \nu_\tau$ is estimated to be 1.4×10^{-4} [16].

Assuming isospin symmetry [17] and using other measurements, we can estimate the $\tau^- \rightarrow \pi^- K_S^0 K_L^0 \nu_\tau$ branching fraction. The $\tau^- \rightarrow \pi^- K^0 \bar{K}^0 \nu_\tau$ and $\tau^- \rightarrow \pi^- K^+ K^- \nu_\tau$ branching fractions are equal if isospin is an exact symmetry (the $\tau^- \rightarrow \pi^- K_S^0 K_S^0 \nu_\tau$ and $\tau^- \rightarrow \pi^- K_L^0 K_L^0 \nu_\tau$ branching fractions are also equal). Hence $B(\tau^- \rightarrow \pi^- K_S^0 K_L^0 \nu_\tau) = B(\tau^- \rightarrow \pi^- K^+ K^- \nu_\tau) - 2B(\tau^- \rightarrow \pi^- K_S^0 K_S^0 \nu_\tau)$ and we obtain

$$B(\tau^- \rightarrow \pi^- K_S^0 K_L^0 \nu_\tau) = (9.8 \pm 0.5) \times 10^{-4}$$

TABLE II. Results for the charged kaon decays. The background events are primarily $q\bar{q}$ events.

Decay mode	$\tau^- \rightarrow K^- K_S^0 K_S^0 \nu_\tau$	$\tau^- \rightarrow K^- K_S^0 K_S^0 \pi^0 \nu_\tau$
Branching fraction	$(1.9 \pm 3.0 \pm 0.3) \times 10^{-7}$	$(1.5 \pm 1.8 \pm 0.1) \times 10^{-7}$
Limit (90% CL)	6.3×10^{-7}	4.0×10^{-7}
Events		
Data	23	1
Estimated background	20.0 ± 0.5	0.15 ± 0.02
Selection efficiency	$(3.85 \pm 0.04)\%$	$(1.37 \pm 0.03)\%$

where $B(\tau^- \rightarrow \pi^- K^+ K^- \nu_\tau) = (14.4 \pm 0.4) \times 10^{-4}$ [2] based on measurements from *BABAR* [18] and Belle [19]. The prediction is in good agreement with the branching fraction measured by ALEPH of $(10.1 \pm 2.3 \pm 1.3) \times 10^{-4}$ [3].

The $(\pi^- K_S^0)$ invariant mass distribution for events that pass the $\tau^- \rightarrow \pi^- K_S^0 K_S^0 \pi^0 \nu_\tau$ selection show evidence for K^{*0} peak (see Fig. 3). The $(\pi^0 K_S^0)$ invariant mass has an excess near $0.9 \text{ GeV}/c^2$ in data with respect to the MC simulation suggesting that K^{*0} mesons may also contribute to this decay. We model the $\tau^- \rightarrow \pi^- K_S^0 K_S^0 \pi^0 \nu_\tau$ decay using $\tau^- \rightarrow K^{*0} K^0 \pi^0 \nu_\tau$ and $\tau^- \rightarrow K^{*0} K^0 \pi^- \nu_\tau$ because a model based on a phase space distribution of the final state particles does not describe the $(\pi^- K_S^0)$ invariant mass distribution. The relative contribution of $\tau^- \rightarrow K^{*0} K^0 \pi^0 \nu_\tau$ to $\tau^- \rightarrow K^{*0} K^0 \pi^- \nu_\tau$ decays is determined to be (0.17 ± 0.03) by simultaneously fitting the $(\pi^- K_S^0)$ and $(\pi^0 K_S^0)$ invariant mass distributions (see Fig. 3). The predicted Monte Carlo distributions are fit to the data spectra after the subtraction of the $\tau^- \rightarrow \pi^- K_S^0 K_S^0 \nu_\tau$ and background events. The normalizations of the two modes are varied with the constraint that the values be positive numbers. If we do not include the $\tau^- \rightarrow K^{*0} K^0 \pi^- \nu_\tau$ decay, then we observe a disagreement between the data and MC samples in the lower-mass and higher-mass regions of the $M(\pi^- K_S^0)$ and $M(\pi^0 K_S^0)$ distributions in Fig. 3.

The same criteria are used to select $\tau^- \rightarrow K^- K_S^0 K_S^0 \nu_\tau$ and $\tau^- \rightarrow K^- K_S^0 K_S^0 \pi^0 \nu_\tau$ decays except that the charged track is required to be a kaon. The numbers of events are given in Table II and found to be consistent with the estimated background prediction. The background is almost entirely due to cross feed of $\tau^- \rightarrow \pi^- K_S^0 K_S^0 \nu_\tau$ and $\tau^- \rightarrow \pi^- K_S^0 K_S^0 \pi^0 \nu_\tau$ decays and very little background from $q\bar{q}$ events. The branching fractions are determined for each channel independently and used to place upper limits on the branching fractions of

$$B(\tau^- \rightarrow K^- K_S^0 K_S^0 \nu_\tau) < 6.3 \times 10^{-7},$$

$$B(\tau^- \rightarrow K^- K_S^0 K_S^0 \pi^0 \nu_\tau) < 4.0 \times 10^{-7},$$

at the 90% confidence level.

The $\tau^- \rightarrow K^- K^0 \bar{K}^0 \nu_\tau$ and $\tau^- \rightarrow K^- K^+ K^- \nu_\tau$ branching fractions are also predicted to be equal assuming isospin symmetry. The $\tau^- \rightarrow K^- K^+ K^- \nu_\tau$ branching fraction is $(2.1 \pm 0.8) \times 10^{-5}$ [2] based on measurements from

BABAR [18] and Belle [19]. *BABAR* finds that a $\tau^- \rightarrow K^- \phi \nu_\tau$ contribution can account for all of the $\tau^- \rightarrow K^- K^+ K^- \nu_\tau$ decays. This suggests that the $\tau^- \rightarrow K^- K_S^0 K_S^0 \nu_\tau$ and, consequently, the $\tau^- \rightarrow K^- K_S^0 K_S^0 \pi^0 \nu_\tau$ branching fractions should be small in the limit of isospin symmetry.

In summary, we have measured the branching fractions of the $\tau^- \rightarrow \pi^- K_S^0 K_S^0 \nu_\tau$ and $\tau^- \rightarrow \pi^- K_S^0 K_S^0 \pi^0 \nu_\tau$ decays to be $(2.31 \pm 0.04 \pm 0.08) \times 10^{-4}$ and $(1.60 \pm 0.20 \pm 0.22) \times 10^{-5}$, respectively. The $\tau^- \rightarrow \pi^- K_S^0 K_S^0 \nu_\tau$ decay can be modeled with $\tau^- \rightarrow K^{*0} K^0 \nu_\tau$, and the $\tau^- \rightarrow \pi^- K_S^0 K_S^0 \pi^0 \nu_\tau$ decay can be modeled with $\tau^- \rightarrow K^{*0} K^0 \pi^0 \nu_\tau$ and $\tau^- \rightarrow K^{*0} K^0 \pi^- \nu_\tau$. The $\tau^- \rightarrow \pi^- K_S^0 K_S^0 \nu_\tau$ branching fraction is a significant improvement on the previous measurements and the $\tau^- \rightarrow \pi^- K_S^0 K_S^0 \pi^0 \nu_\tau$ branching fraction is the first measurement. In addition, we place the first upper limits on the branching fractions of 6.3×10^{-7} and 4.0×10^{-7} on the $\tau^- \rightarrow K^- K_S^0 K_S^0 \nu_\tau$ and $\tau^- \rightarrow K^- K_S^0 K_S^0 \pi^0 \nu_\tau$ decay modes at the 90% confidence level.

We are grateful for the extraordinary contributions of our PEP-II colleagues in achieving the excellent luminosity and machine conditions that have made this work possible. The success of this project also relies critically on the expertise and dedication of the computing organizations that support *BABAR*. The collaborating institutions wish to thank SLAC for its support and the kind hospitality extended to them. This work is supported by the U.S. Department of Energy and National Science Foundation, the Natural Sciences and Engineering Research Council (Canada), the Commissariat à l'Énergie Atomique and Institut National de Physique Nucléaire et de Physique des Particules (France), the Bundesministerium für Bildung und Forschung and Deutsche Forschungsgemeinschaft (Germany), the Istituto Nazionale di Fisica Nucleare (Italy), the Foundation for Fundamental Research on Matter (The Netherlands), the Research Council of Norway, the Ministry of Education and Science of the Russian Federation, Ministerio de Ciencia e Innovación (Spain), and the Science and Technology Facilities Council (United Kingdom). Individuals have received support from the Marie-Curie IEF program (European Union) and the A.P. Sloan Foundation (USA).

- [1] J. P. Lees *et al.* (BABAR Collaboration), *Phys. Rev. D* **85**, 031102 (2012).
- [2] J. Beringer *et al.* (Particle Data Group), *Phys. Rev. D* **86**, 010001 (2012).
- [3] R. Barate *et al.* (ALEPH Collaboration), *Eur. Phys. J. C* **4**, 29 (1998).
- [4] T. E. Coan *et al.* (CLEO Collaboration), *Phys. Rev. D* **53**, 6037 (1996).
- [5] B. Aubert *et al.* (BABAR Collaboration), *Nucl. Instrum. Methods Phys. Res., Sect. A* **479**, 1 (2002).
- [6] S. Jadach, B. F. L. Ward, and Z. Wąs, *Comput. Phys. Commun.* **130**, 260 (2000).
- [7] S. Jadach, Z. Wąs, R. Decker, and J. Kühn, *Comput. Phys. Commun.* **76**, 361 (1993).
- [8] D. J. Lange, *Nucl. Instrum. Methods Phys. Res., Sect. A* **462**, 152 (2001).
- [9] T. Sjöstrand, *Comput. Phys. Commun.* **82**, 74 (1994).
- [10] E. Barberio and Z. Wąs, *Comput. Phys. Commun.* **79**, 291 (1994).
- [11] S. Agostinelli *et al.* (Geant4 Collaboration), *Nucl. Instrum. Methods Phys. Res., Sect. A* **506**, 250 (2003).
- [12] S. Brandt, Ch. Peyrou, R. Sosnowski, and A. Wroblewski, *Phys. Lett.* **12**, 57 (1964); E. Farhi, *Phys. Rev. Lett.* **39**, 1587 (1977).
- [13] J. P. Lees *et al.* (BABAR Collaboration), *Phys. Rev. D* **81**, 111101(R) (2010).
- [14] A. Stahl, *Springer Tracts in Modern Physics* (Springer-Verlag, Berlin, 2000), Vol. 160.
- [15] B. Aubert *et al.* (BABAR Collaboration), *Phys. Rev. Lett.* **99**, 021603 (2007).
- [16] M. Finkemeier and E. Mirkes, *Z. Phys. C* **69**, 243 (1996); M. Finkemeier, J. Kühn, and E. Mirkes, *Nucl. Phys. B, Proc. Suppl.* **55**, 169 (1997).
- [17] A. Rouge, *Z. Phys. C* **70**, 65 (1996).
- [18] B. Aubert *et al.* (BABAR Collaboration), *Phys. Rev. Lett.* **100**, 011801 (2008).
- [19] M. J. Lee *et al.* (Belle Collaboration), *Phys. Rev. D* **81**, 113007 (2010).